AIP | Applied Physics Letters

# Electric-field-tunable defect mode in one-dimensional photonic crystal operating in the terahertz range

V. Skoromets, H. Němec, C. Kadlec, D. Fattakhova-Rohlfing, and P. Kužel

Citation: Appl. Phys. Lett. **102**, 241106 (2013); doi: 10.1063/1.4809821
View online: http://dx.doi.org/10.1063/1.4809821
View Table of Contents: http://apl.aip.org/resource/1/APPLAB/v102/i24
Published by the AIP Publishing LLC.

# Electric-field-tunable defect mode in one-dimensional photonic crystal operating in the terahertz range

V. Skoromets,[1] H. Němec,[1] C. Kadlec,[1] D. Fattakhova-Rohlfing,[2] and P. Kužel[1,a)]
[1]*Institute of Physics, Academy of Sciences of the Czech Republic, Prague, Na Slovance 2, CZ-18221, Czech Republic*
[2]*Department of Chemistry, University of Munich (LMU), Munich, Butenandtstrasse 5-11 (E), D-81377, Germany*

(Received 30 April 2013; accepted 22 May 2013; published online 18 June 2013)

A one-dimensional photonic crystal possessing an electric-field-tunable defect mode in the lowest forbidden band is demonstrated. The compact photonic structure consists of two symmetric Bragg mirrors made of alternate quarter-wave layers of $SiO_2$ and $CeO_2$ separated by a defect layer of an incipient ferroelectric $SrTiO_3$ with electrodes transparent for terahertz radiation on its both sides. The applied bias is then perpendicular to the layer and modifies the in-plane dielectric function, which is probed by the transverse terahertz wave. The observed tunable behavior is in agreement with the model of the ferroelectric soft mode behavior in $SrTiO_3$ single crystals. The defect-mode frequency tunability is proportional to that of the soft mode: we achieved a relative tunability of 6.5% at 105 K under an electric bias of 60 kV/cm.  [http://dx.doi.org/10.1063/1.4809821]

Photonic crystals (PCs) are periodic structures which can exhibit forbidden frequency bands[1,2] in which they do not transmit electromagnetic radiation. Breaking of their periodicity usually results in a narrow transmission spectral line in the forbidden band, which is called a defect mode.[3] The field distribution of the defect mode shows a strong confinement in the proximity of the defect layer.[4,5] These properties make PCs attractive for a number of applications like narrow passband filters,[3] resonant cavities with a high quality factor,[6] waveguides,[7,8] and couplers designed to enhance nonlinear phenomena.[9]

The tuning of the defect mode frequency is an interesting possibility to enhance the application potential of photonic structures; this may be achieved by changing the operating temperature,[10–13] by applying an external magnetic[14–17] and/or electric field,[18–22] or by optical illumination.[23,24] Obviously, the most promising way to control the defect mode consists in applying a voltage, as it is easy to implement. Most works on the electric-field tunability of the defect mode are either theoretical or targeted to the optical spectral range; whereas no experimentally demonstrated prototype of PCs with an electrically tunable defect mode in the terahertz (THz) frequency range have been reported so far. The THz frequency region is of particular interest, because beside its spectroscopic use, it provides interesting possibilities in imaging, sensing, and communication technologies.[25]

In this Letter, we propose and experimentally characterize a one-dimensional (1D) PC for the THz frequency range with an electric-field-tunable defect mode. The tunable properties originate from the anharmonic lattice behavior of the incipient ferroelectric $SrTiO_3$ (STO) single crystal,[26] which is inserted into the PC as the defect layer.

The investigated PC shows a twin defect (Fig. 1), i.e., the defect layer is enclosed between two identical Bragg mirrors consisting of two alternating dielectric layers. Several facts should be taken into account for the design of Bragg mirrors. First, a higher reflectance of the mirrors implies a stronger feedback and, consequently, a narrower defect mode and higher transmission losses in a lossy defect layer. A compromise should be found between a high peak transmission and an acceptable width of the defect mode. Second, the lowest forbidden band of the PC should be as broad as possible. This is achieved when the alternating layers composing the Bragg mirror have equal optical thicknesses[27] and when the contrast of refractive indices of the layers is high ($n_H/n_L \approx 2.3$ in our case). Finally, it was shown that the widest tunability of the structure, where the refractive index of the defect ($n_D$) is high ($n_D \gg n_L,\ n_H$), is achieved when the defect layer is surrounded by the low-index ($n_L$) layers.[5]

In our study, we used the Bragg mirrors previously employed for the investigation of a thermally tunable defect mode in a 1D PC.[12] Crystalline quartz was used as the low-index material ($n_L \approx 2.1$), and undoped $CeO_2$ ceramic played the role of the high-index material ($n_H \approx 4.8$). This ceramic shows low losses in the THz range, and its permittivity is almost temperature independent.[28] All individual layers forming the Bragg mirrors were polished to optical quality on both surfaces. Each mirror was made of three quartz plates (each 230 $\mu$m thick) separated by two discs of $CeO_2$ ceramic (each 100 $\mu$m thick). The clear aperture of the Bragg mirrors was larger than 8 mm.

STO single crystal was purchased from Crystal GmbH and thinned down to a thickness $d_D = 50\ \mu$m. The geometrical dimensions of the crystal used as the defect layer were $10 \times 10 \times 0.05$ mm$^3$. On both sides of the plate, we deposited nanocrystalline Sb-doped $SnO_2$ films with a thickness of ~200 nm (Fig. 1).[26] These thin-film electrodes combine a sufficient low-frequency (MHz) conductivity and transparency in the THz range. The details on the synthesis and deposition of the doped $SnO_2$ nanoparticles were published elsewhere.[26,29] The areas

a)Author to whom correspondence should be addressed. Electronic mail: kuzelp@fzu.cz

 

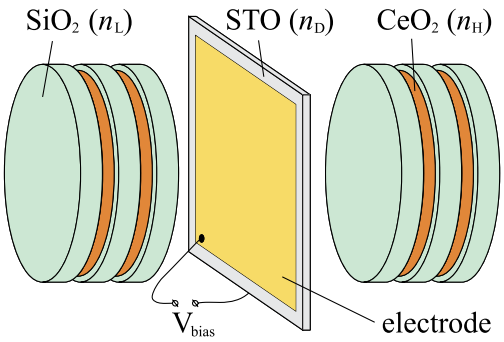


FIG. 1. Scheme of the investigated photonic crystal with $SrTiO_3$ (STO) single crystal as a defect layer.

covered by the thin-film electrodes were $\sim 8 \times 8$ mm$^2$ on both surfaces of the crystal. Before assembling the PC, thin electrical wires were put in contact with corners of both electrode-film square patterns by a high-purity silver paint. The RC constant of the crystal with electrodes was theoretically estimated to be about 20 $\mu$s (the capacitance of STO slab is $\sim$10 nF at 105 K and the resistance of electrodes is $\sim$2 k$\Omega$). The entire structure consisting of two Bragg mirrors and the defect was enclosed between two apertures and tightened with screws.

The dielectric response of STO in the THz range is governed by the ferroelectric soft mode (SM)[30,31] which has a strongly polar character. Its contribution to the sub-THz permittivity is given by

$$\Delta\varepsilon = \frac{f}{\omega_0^2(T,E)} \quad (1)$$

where $\omega_0$ is the soft mode frequency and $f$ is its oscillator strength, which is proportional to the square of the effective charge connected to this vibrational degree of freedom. The SM frequency is markedly temperature ($T$) dependent due to the proximity of the lattice instability (ferroelectric phase transition) and its electric field ($E$) dependence is connected to the anharmonicity of the lattice potential.[32] The latter becomes more anharmonic at lower temperatures with approaching to the ferroelectric phase transition. This is illustrated in Fig. 2 where the dielectric spectra of STO with and without electric field are plotted for 105, 150, and 300 K; the curves are based on the data published in Ref. 26.

A custom-made time-domain THz spectrometer[33] arranged in the transmission geometry was used for experimental study of an electric-field-tunable defect mode in the temperature range from 90 to 300 K. The entire photonic structure was put in a helium-cooled cryostat equipped with electrical connections for the bias field application. Transmitted time-domain THz signal was measured for each applied field value and each temperature. A reference measurement was made with an empty aperture. The complex transmission spectra were then calculated as ratios of the Fourier transformations of the signal and reference wave forms. The time-domain scans were 250 ps long, which corresponds to a spectral resolution of 4 GHz.

The measured transmission functions at 105 K and 150 K are shown in Fig. 3 in the frequency range corresponding to the lowest forbidden band together with calculations based on transfer matrix formalism.[34] The lowest forbidden band lies

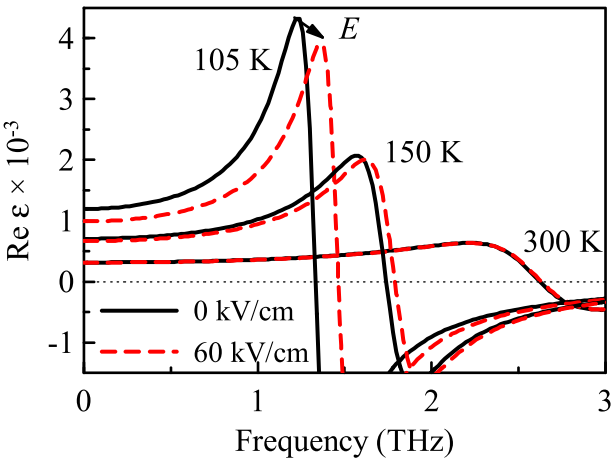


FIG. 2. Calculated dielectric spectra of STO single crystal with and without applied electric field based on data from Ref. 26.

between 100 and 215 GHz at 105 K and it contains a single defect mode (at $\sim$173 GHz for 0 kV/cm). Upon application of the electric field, the defect-mode transmission peak shifts towards higher frequencies and its amplitude increases. This behavior directly stems from the properties of STO, where the applied field leads to a decrease of the permittivity (see Fig. 2) and losses.[26] The observed defect-mode frequency shift under the maximum applied field of 60 kV/cm is 11.5 GHz, the defect-mode linewidth is $\sim$8 GHz and the peak transmission is about $-16$ dB. The relative tunability defined as a ratio of the tuning range and the central frequency then reaches 6.5%.

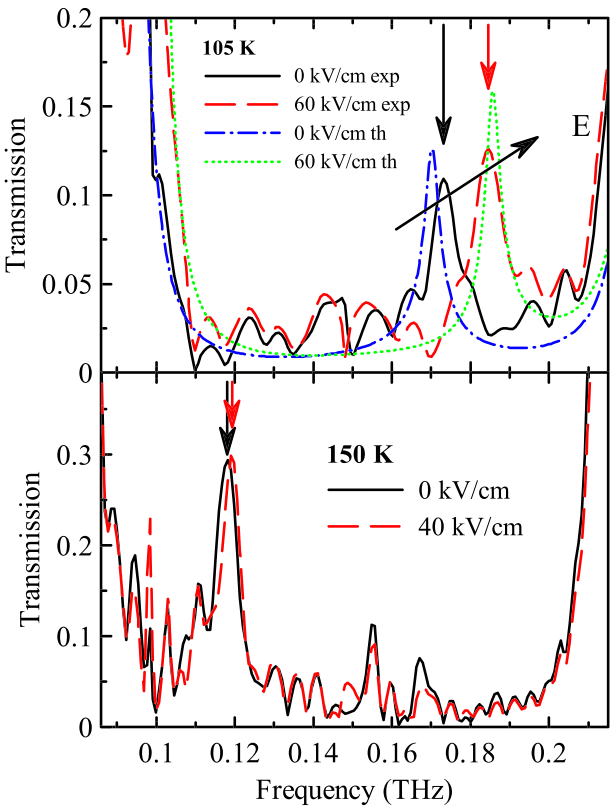


FIG. 3. Amplitude transmissions of the investigated PC in the frequency range of the first forbidden band at 105 K (upper panel) and 150 K (lower panel): solid (0 kV/cm) and dashed (60 kV/cm) curves are measured spectra; dashed-dotted (0 kV/cm) and dotted (60 kV/cm) curves were calculated by transfer-matrix formalism using complex dielectric function of STO taken from Ref. 26.

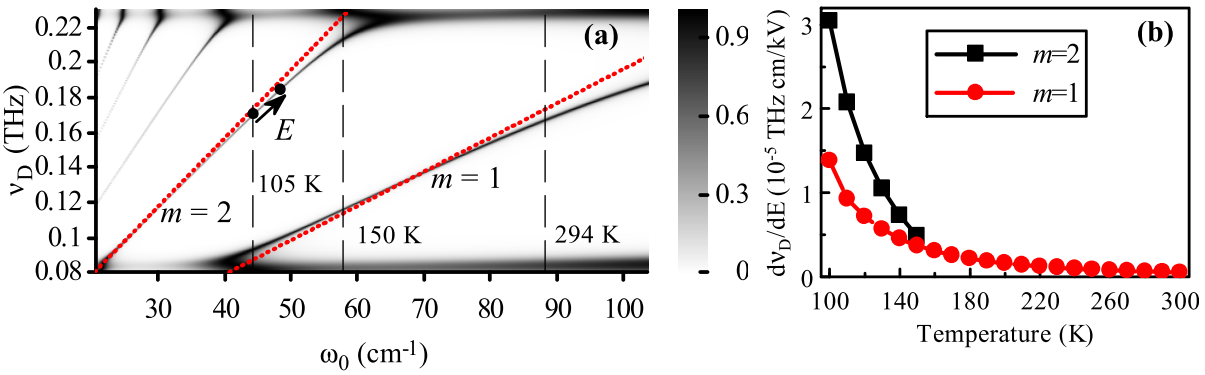


FIG. 4. (a) Calculated frequency of the defect modes in the first forbidden band versus the soft mode frequency in 50-$\mu$m-thick STO defect layer (losses of STO are neglected in this figure). The grayscale indicates the power transmittance of the PC. Dashed lines show the soft mode frequencies at 105, 150, and 294 K. The two solid symbols on the second order branch indicate the tunability achieved by an electric field $E = 60$ kV/cm at 105 K. The red dotted lines correspond to the approximate linear relation (2). (b) Calculated temperature dependence of the field tunability of the defect mode: $d\nu_D/dE$.

Using the transfer matrix method, we calculated a series of transmission spectra of the PC in the lowest forbidden band with $n_D$ obtained from the STO permittivity[35] and neglecting the losses; the results are shown in Fig. 4.

The soft mode contribution to the permittivity $\Delta\varepsilon$ of STO is largely dominant (>96% below room temperature) over the high-frequency one which is due to hard polar phonon modes and electronic polarization. In this sense, the soft mode fully determines the dielectric function and the refractive index $n_D$ in the THz and sub-THz range and it is possible to relate the defect mode frequency $\nu_D$ to the soft mode frequency $\omega_0$ (Fig. 4). An analytical formula can be also derived from Eq. (25) in Ref. 35 and with an assumption that $n_D \approx \sqrt{\Delta\varepsilon}$; we show here an approximation valid close to the center of the bandgap, where the reflectance phase of the Bragg mirrors can be neglected

$$\nu_D(T,E) \approx \frac{mc}{2\sqrt{f}\,d_D}\omega_0(T,E). \qquad (2)$$

Here $c$ is the speed of light in vacuum and $m$ is an integer denoting the defect mode order. This relation implies a linear dependence between $\nu_D$ and $\omega_0$. Fig. 4 clearly shows that Eq. (2) constitutes a very good approximation of the defect mode behavior. At 105 K we observe the defect mode with $m = 2$. Its tunability is increased by a factor of 2 compared to the defect modes on the branch $m = 1$, as for example that observed at 150 K and shown in Fig. 3. The defect mode frequency is inversely proportional to the defect layer thickness; it means that the tunability of the structure increases with decreasing $d_D$. Note, however, that for some value of the thickness, the defect mode will merge with the allowed frequency band at the high-frequency edge of the bandgap. Another mode with a lower $m$ (and lower tunability) will enter into the forbidden band.

There is a good agreement between the measured spectra and the transmission calculated by the transfer matrix formalism (Fig. 3). One can note a small frequency shift between the theoretical and experimental data, which may originate from an uncertainty of the structural parameters of the PC. Furthermore, the theoretically predicted tunability (~10%) is somewhat larger than the measured one (~6.5%). There are two possible sources of this reduced tunability. Since we used mechanical polishing of a thick STO single crystal to prepare the very thin plate inserted into the PC, a residual stress affecting the lattice dynamics of STO may be produced.[36] This may change not only the steady-state (unbiased) dielectric properties, but also the electric-field tunability via the soft polar mode dynamics.[26] In other words, the dielectric properties of the 50-$\mu$m-thick crystals can slightly differ from one sample to another. In addition, a possible partial damage of the thin-film tin oxide electrodes during the construction of the PC can be at the origin of the observed lower tunability. Indeed, defects in the percolation of the conductive film and possible existence of small electrically isolated areas would decrease the surface of the sample influenced by the bias.

In Fig. 5, we summarize the defect mode tuning as a function of the electric field and we show also the data up to the second forbidden band, which spreads from ~400 to ~530 GHz. One can distinguish two rather weak ($\leq -30$ dB) defect modes in the second band gap. The first one splits out from the lower band edge at about 20 kV/cm and shifts up to 450 GHz at $E = 60$ kV/cm. The second one is hard to distinguish at zero field: it starts at about 480 GHz and it merges with the upper band edge for electric field of 60 kV/cm. The relative tunability of these modes is about 10%, which is comparable to that of the defect mode in the first forbidden band. However, their peak transmission is too low to be of interest in potential applications.

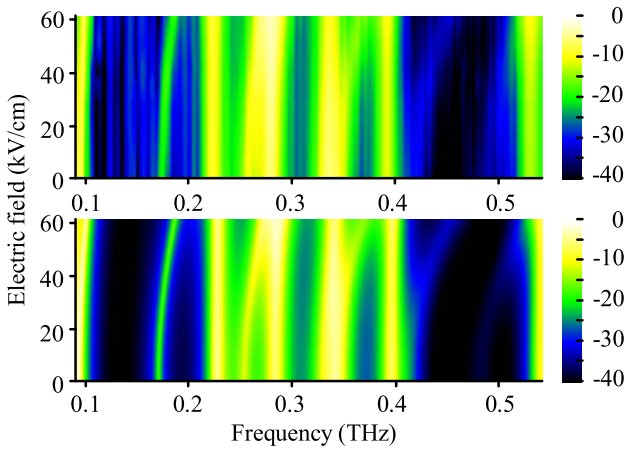


FIG. 5. Transmission spectra at 105 K up to the second forbidden band. Upper panel—measured data; lower panel—calculation by transfer matrix formalism. The color scale indicates the transmittance expressed in dB.

The electric-field tunability of STO decreases with increasing temperature (see Fig. 2), but the losses in STO become lower, too. Consequently, at higher temperature a better peak transmission of the defect mode is observed, which is paid by its lower tunability. For example, the peak transmission of the defect mode at 150 K exceeds −9 dB, but its relative tunability drops to ∼1% at 40 kV/cm (see Fig. 3, lower panel). At 120 K, the tunability is about 2% but the transmission peak reduces to −13 dB. Cooling the PC below 105 K is not reasonable because of a significant reduction of the defect-mode peak transmission related to rapidly increasing dielectric losses in STO. Moreover, a ferroelastic cubic-to-tetragonal phase transition at 105 K would lead to an anisotropy of dielectric properties of STO crystals at lower temperatures.[37]

To summarize, we have demonstrated an electric-field-tunable defect mode in the first forbidden band of a 1D PC. The relative tunability of 6.5% was achieved at 105 K under the applied electric field value of 60 kV/cm. The tunability originates from the electric-field-dependent permittivity of a $SrTiO_3$ crystal embedded as a defect in the 1D PC. The frequency of the defect mode scales linearly with the frequency of the ferroelectric soft mode of $SrTiO_3$.

The financial support by the Czech Science Foundation (Grant No. 13-12386S) and by the Academy of Sciences of the Czech Republic (project M100101218) is acknowledged.

[1]K. Sakoda, *Optical Properties of Photonic Crystals* (Springer-Verlag, Berlin, 2001).
[2]E. Yablonovitch, Phys. Rev. Lett. **58**, 2059 (1987).
[3]E. Yablonovitch, T. G. Gmitter, R. D. Meade, A. M. Rappe, K. D. Brommer, and J. D. Joannopoulos, Phys. Rev. Lett. **67**, 3380 (1991).
[4]S. L. McCall, P. M. Platzman, R. Dalichaouch, D. Smith, and S. Schultz, Phys. Rev. Lett. **67**, 2017 (1991).
[5]H. Němec, L. Duvillaret, F. Quemeneur, and P. Kužel, J. Opt. Soc. Am. B **21**, 548 (2004).
[6]Y. Akahane, T. Asano, B.-S. Song, and S. Noda, Nature **425**, 944 (2004).
[7]S.-Y. Lin, E. Chow, V. Hietala, P. R. Villeneuve, and J. D. Joannopoulos, Science **282**, 274 (1998).
[8]B. Temelkuran and E. Özbay, Appl. Phys. Lett. **74**, 486 (1999).
[9]C. M. Bowden and A. M. Zheltikov, J. Opt. Soc. Am. B **19**, 2046–2048 (2002).
[10]B. Wild, R. Ferrini, R. Houdré, M. Mulot, S. Anand, and C. J. M. Smith, Appl. Phys. Lett. **84**, 846 (2004).
[11]H. Němec, L. Duvillaret, F. Garet, P. Kužel, P. Xavier, J. Richard, and D. Rauly, J. Appl. Phys. **96**, 4072 (2004).
[12]H. Němec, P. Kužel, L. Duvillaret, A. Pashkin, M. Dressel, and M. T. Sebastian, Opt. Lett. **30**, 549 (2005).
[13]H.-C. Hung, C.-J. Wu, and S.-J. Chang, J. Appl. Phys. **110**, 093110 (2011).
[14]H. Tian and J. Zi, Opt. Commun. **252**, 321 (2005).
[15]C.-Y. Chen, C.-L. Pan, C.-F. Hsied, Y.-F. Lin, and R.-P. Pan, Appl. Phys. Lett. **88**, 101107 (2006).
[16]C.-L. Pan, C.-F. Hsieh, R.-P. Pin, M. Tanaka, F. Miyamaru, M. Tani, and M. Hangyo, Opt. Express **13**, 3921 (2005).
[17]M. Inoue, R. Fujikawa, A. Baryshev, A. Khanikaev, P. B. Lim, H. Uchida, O. Aktsipetrov, A. Fedyanin, T. Murzina, and A. Granovsky, J. Phys. D: Appl. Phys. **39**, R151 (2006).
[18]Q. Zhu and Y. Zhang, Optik **120**, 195 (2009).
[19]P. Halevi, J. A. Reyes-Avendano, and J. A. Reyes-Cervantes, Phys. Rev. E **73**, 040701(R) (2006).
[20]Y. S. Kim, S.-Y. Lin, H.-Y. Wu, and R.-P. Pan, J. Appl. Phys. **109**, 123111 (2011).
[21]R. Ozaki, T. Matsui, M. Ozaki, and K. Yoshino, Jpn. J. Appl. Phys., Part 2 **41**, L1482 (2002).
[22]R. Ozaki, T. Matsui, M. Ozaki, and K. Yoshino, Appl. Phys. Lett. **82**, 3593 (2003).
[23]D. McPhail, M. Straub, and M. Gu, Appl. Phys. Lett. **87**, 091117 (2005).
[24]L. Fekete, F. Kadlec, H. Němec, and P. Kužel, Opt. Express **15**, 8898 (2007).
[25]M. Tonouchi, Nature Photon. **1**, 97 (2007).
[26]V. Skoromets, F. Kadlec, C. Kadlec, H. Němec, I. Rychetsky, G. Panaitov, V. Müller, D. Fattakhova-Rohlfing, P. Moch, and P. Kužel, Phys. Rev. B **84**, 174121 (2011).
[27]J. N. Winn, Y. Fink, S. Fan, and J. D. Joannnopoulos, Opt. Lett. **23**, 1573 (1998).
[28]N. I. Santha, M. T. Sebastian, P. Mohanan, N. M. Alford, K. Sarma, R. C. Pullar, S. Kamba, A. Pashkin, P. Samukhina, and J. Petzelt, J. Am. Ceram. Soc. **87**, 1233 (2004).
[29]V. Müller, M. Rasp, G. Stefanic, J. Ba, S. Gunther, and J. Rathousky, Chem. Mater. **21**, 5229 (2009).
[30]R. A. Cowley, Phys. Rev. **134**, A981 (1964).
[31]J. Hlinka, J. Petzelt, S. Kamba, D. Noujni, and T. Ostapchuk, Phase Transitions **79**, 41 (2006).
[32]C. Kadlec, V. Skoromets, F. Kadlec, H. Němec, J. Hlinka, J. Schubert, G. Panaitov, and P. Kužel, Phys. Rev. B **80**, 174116 (2009).
[33]P. Kužel, H. Němec, F. Kadlec, and C. Kadlec, Opt. Express **18**, 15338 (2010).
[34]R. Jacobsson, in *Progress in Optics*, edited by E. Wolf (North-Holland, 1965), Chap. 5, pp. 255–258.
[35]P. Kužel and F. Kadlec, C. R. Phys. **9**, 197–214 (2008).
[36]K. Aso, Jpn. J. Appl. Phys., Part 1 **15**, 1243 (1976).
[37]T. Sakudo and H. Unoki, Phys. Rev. Lett. **26**, 851 (1971).